

Jörn H. Kruhl

## Crystallographic control on the development of foam textures in quartz, plagioclase and analogue material

Received: 25 October 1999 / Accepted: 9 October 2000 / Published online: 22 March 2001  
© Springer-Verlag 2001

**Abstract** The shape, pattern and crystallographic orientation of grain boundaries represent important characteristics of crystalline material and contain information about its deformation and annealing history. The present study includes measurements of grain boundaries from experimentally annealed analogue material as well as natural foam texture of quartz and plagioclase. The main subject is the relation between the development of a foam texture and the crystallographic orientation of its grain boundaries and their geometry. (1) During annealing, grain sizes stabilize at certain values. On a statistical basis, these values can be applied as a geothermometer. (2) On the light-microscope scale, the grain boundaries in foam textures commonly consist of two or several planar facets. They are preferentially oriented along specific crystallographic planes, namely in relation to both neighbouring crystals; for quartz they tend to be rhombohedral. (3) Even highly misoriented facets and dihedral angles largely deviating from the 'equilibrium angle' of  $120^\circ$  may be stable over long periods of annealing. (4) Parts of single boundaries may migrate, whereas other parts are stationary during annealing. The results of the present study suggest that the anisotropy of surface energy has a considerable influence on the development of foam textures and that modelling of texture development should include the influence of the crystallographic orientation of grain boundaries.

**Keywords** Analogue material · Crystallographic control · Dihedral angle · Foam texture · Grain boundary

### Introduction

The microfabric, i.e. the shape, size and spatial distribution of material domains, is one of the most important sources of information concerning the physical characteristics of natural and artificial crystalline material and the history of its development. Specifically, the microfabric of metamorphic rocks can provide useful information about the tectonometamorphic history of these rocks. Basic parameters such as temperature, stress, strain, and the amount and type of fluids can be inferred from microfabric data. However, because of their complexity and variation, our knowledge about microfabrics and their development is still incomplete. A comparatively simple but quite common situation is represented by fabric development in the absence of differential stress. This typically leads to polygonal grain boundary patterns, commonly termed foam textures (Spry 1969; Kingery et al. 1976). Although foam textures are quite common, they have rarely been investigated in detail (Smith 1948; McLean 1957; Kretz 1966, Vernon 1968). There are recent attempts to study the development of foam textures on the basis of analogue materials (Bons 1994) or theoretical considerations and computer modelling (Humphreys 1997; Jessel et al. 1999).

The present study combines experimental annealing of analogue material with measurements of natural quartz and plagioclase with foam texture. Its main subject is (1) to investigate the question how foam textures and their development during annealing can be characterized, (2) to provide information about the crystallographic control on grain boundary shapes and mobility, and (3) to contribute to the question whether the average grain size in foam textures stabilizes in dependence upon temperature, which has been discussed controversially.

J.H. Kruhl (✉)  
Lehrstuhl für Allgemeine, Angewandte und Ingenieur-Geologie,  
Technische Universität, Arcisstraße 21, 80290 München,  
Germany  
E-mail: joern.kruhl@geo.tum.de

## Grain coarsening during annealing

### Experimental annealing of analogue material

The coarsening of 99%-pure (1R)-(+)-camphor [ $C_{10}H_{16}O$ ] grain aggregates has been studied experimentally. The experiments included the following steps: Camphor was (1) cooled to 5–6 °C (to avoid stickiness of the material) and finely cut with a razor-blade, (2) equally powdered on a plastic foil and pressed for 15–30 s between two metal pistons to produce several mm large ~30–40  $\mu\text{m}$  evenly thick camphor flakes. (3) These flakes with grain sizes of ~10–30  $\mu\text{m}$  were placed side by side on a glass plate and covered by a second glass plate. (4) The two plates were marginally sealed against each other and then (5) mounted on a heating stage that was already at a fixed temperature. (6) After defined time steps microphotographs were taken from specific areas of the camphor sample to document the grain size and grain boundary development. Microphotographs were only taken from regions optically free of bubbles.

The results were influenced by some variations and inaccuracies of the experiments. Mainly during runs at higher temperatures some material domains slightly shifted within the area of observation and partly left the area of measurement. This probably is the reason for the slight variation of the average grain sizes and their confidence intervals after reaching the 'stabilized' grain size (Fig. 1). Prior to the runs, the powder was pressed at room temperature for varying periods. The pressure was kept qualitatively but not quantitatively at the same level. This could have resulted in slightly different grain sizes at the beginning of each run.

At room temperature camphor is orthorhombic; it changes to the cubic state above 90–100 °C (depending on the exact composition; Yager and Morgan 1935) and melts at ~179 °C (Dean 1985). The experiments were performed between 18 and 90 °C, i.e. with orthorhombic camphor, with annealing periods of up to 3 days, which led to polygonal grain aggregates (foam

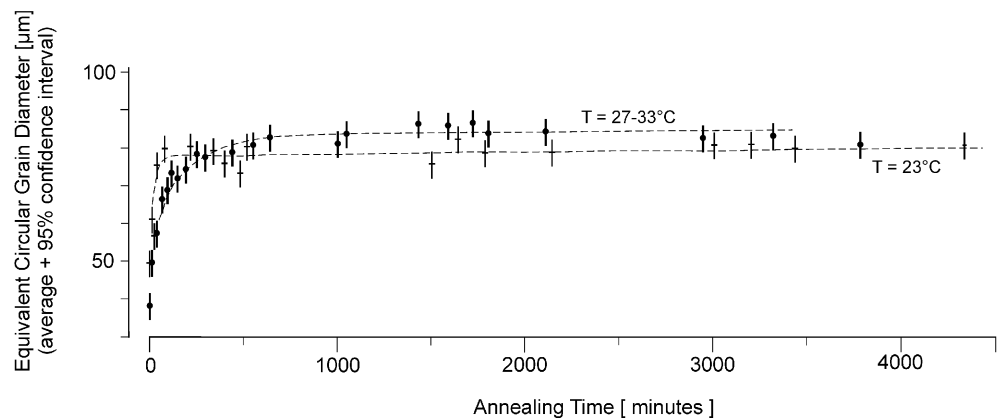
textures). Continuous checks with a gypsum test plate proved the absence of a preferred crystallographic orientation in the foam textures at any time of the runs, including the start after cold pressing.

Figure 1 shows the general grain-size development of the foam textures in regions free of bubbles from two different samples. The grain size undergoes an initial rapid increase but then it slows and finally stays constant within 95% confidence intervals. The periods of rapid and slow increase in grain size can be compared with periods of primary recrystallization and normal grain growth described by Olgaard and Evans (1986) for the grain-size evolution during experimental annealing of calcite powder. In general, the stable grain size is more rapidly reached at higher temperatures. The presence of bubbles strongly inhibits grain growth. In those regions optically free of bubbles the stable average grain size roughly increases with annealing temperature (Fig. 2).

### Grain coarsening caused by annealing during regional metamorphism

On a statistical basis the size of recrystallized and coarsened grains correlates well with the temperature of regional metamorphism. On the basis of recrystallized and coarsened plagioclase from two regions with regional metamorphism of different temperature (the southwestern part of the Lepontine temperature dome in the Western Alps and the fossil Hercynian lower crust of Calabria/Italy), an approximately linear relationship between the average grain diameter and the temperature is found (Fig. 3). Even if the average grain diameter at a specific temperature differs for different samples or regions of measurements, the 95% confidence intervals are clearly separated for temperatures ranging from 500 (the approximate start of plagioclase recrystallization; Voll 1976) to nearly 800 °C. The studied plagioclase from both regions has been recrystallized and subsequently annealed during prograde metamorphism up to maximum and during decreasing temperatures (Kruhl 1979; Altenberger et

**Fig. 1** Grain size of camphor foam texture versus duration of annealing. The bars represent the 95% confidence interval of the equivalent circular average grain diameter (diameter of a circle of the same area as the measured grain), determined on the basis of 100–150 measurements. Shown are the results of two runs with different annealing temperatures  $T$ . The dashed lines emphasize the general trend of the grain-size development.



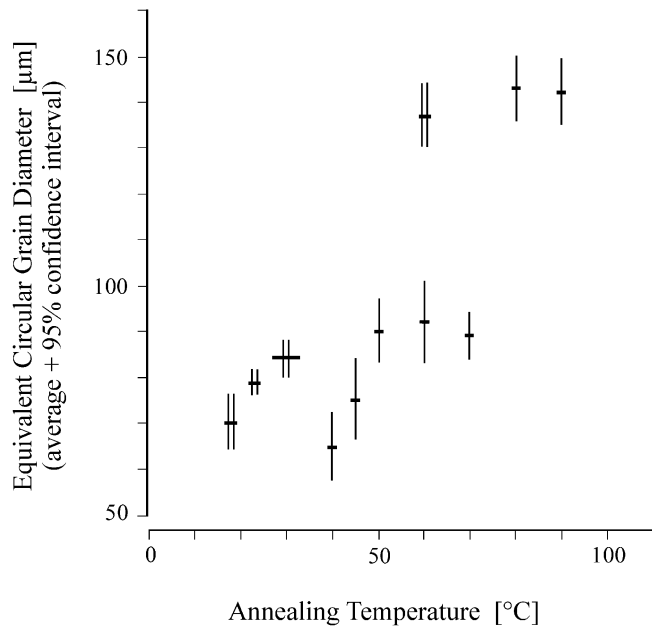


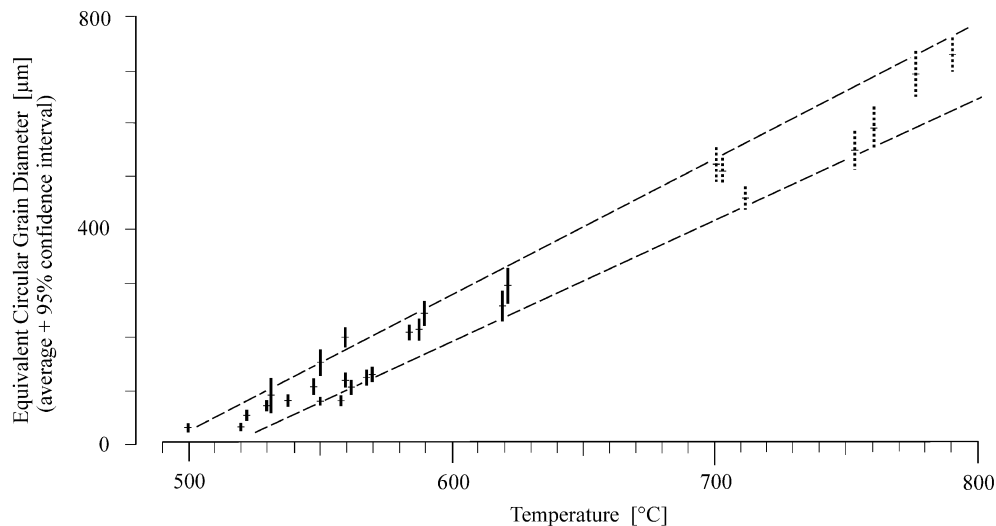
**Fig. 2** Annealing temperature versus equivalent circular average grain diameter of camphor foam textures. 11 runs of ~25 to 70 h duration at different temperatures. *Single bars* indicate ~30 s duration of time of initial loading, *double bars* 15–20 s

al. 1987; Kruhl and Huntemann 1991), resulting in foam textures with equidimensional or nearly equidimensional strain-free grains (Fig. 4A). In the south-western Lepontine temperature dome the duration of annealing above 500 °C is difficult to estimate. Based on white mica cooling in the Alpine ‘Root Zone’ below ~500 °C at ~25–30 Ma (Hunziker et al. 1992) and a supposed maximum of (Meso-Alpine) metamorphism of ~40 Ma, a period of annealing >500 °C of several tens of million years may be inferred. However, this period might be considerably short in regions with maximum temperatures close to 500 °C. The fos-

sil Hercynian lower crust of Calabria cooled during a period of ~50 million years from the granulite facies temperature maximum to 500 °C (Schenk 1990). Because plagioclase recrystallization occurred prior to this maximum (Kruhl and Huntemann 1991), the total period of heating above 500 °C was at least slightly but probably much (up to several 100 million years) longer (see discussion in Schenk 1990).

It is important to note that during the grain size measurements (1) only plagioclase aggregates without any secondary phases have been measured and (2) high-strain zones with an initially higher number of recrystallized grains and, therefore, probably a smaller final grain size have been avoided. Taking these restrictions into account and on a statistical basis, the correlation between average grain diameter and temperature (Fig. 3) may serve as a geothermometer.

**Fig. 3** Annealing temperature versus equivalent circular average grain diameter of recrystallized and subsequently annealed and coarsened plagioclase grains from orthogneisses of the Monte-Rosa and Sesia Zone, Western Alps (*solid lines*; modified after Altenberger et al. 1987) and granulites of the fossil Hercynian lower crust of Calabria, Italy (*broken lines*; Kruhl, unpublished data). Each average diameter is based on 100–150 (in rare cases 50) measurements from one thin section. The frequency distributions of grain diameters follow normal or nearly normal distributions. The maximum temperature for each sample has been estimated on the basis of their localities and the maximum temperatures of regional metamorphism given in the literature. Western Alps: The maximum temperatures are based on the oligoclase boundary, the cloritoid–staurolite transition, and the occurrence of the serpentine–talc–forsterite paragenesis, taken from Altenberger et al. (1987) and Kruhl (1979); Calabria: The distribution of maximum temperatures have been taken from Schenk (1990) who calculated, on the basis of different petrological thermometers, temperatures decreasing from ~800 °C at the lower margin of the fossil Hercynian lower crust of Calabria to ~670 °C at the top



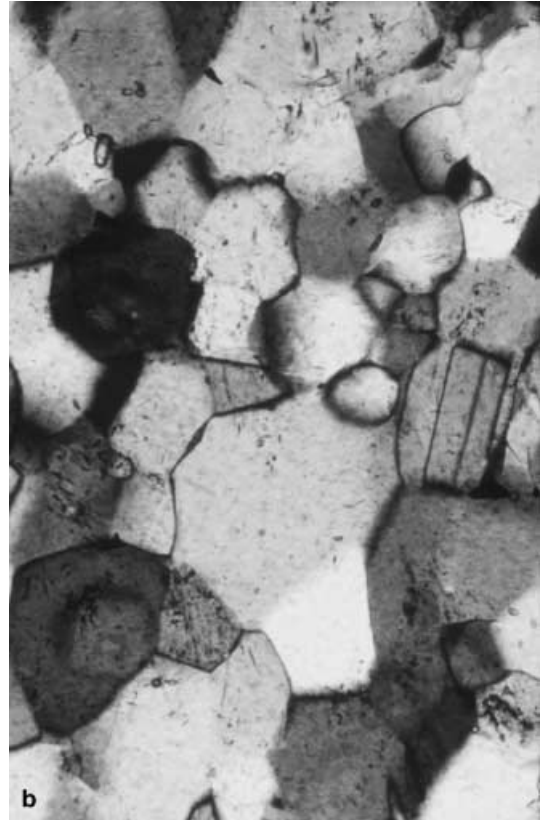
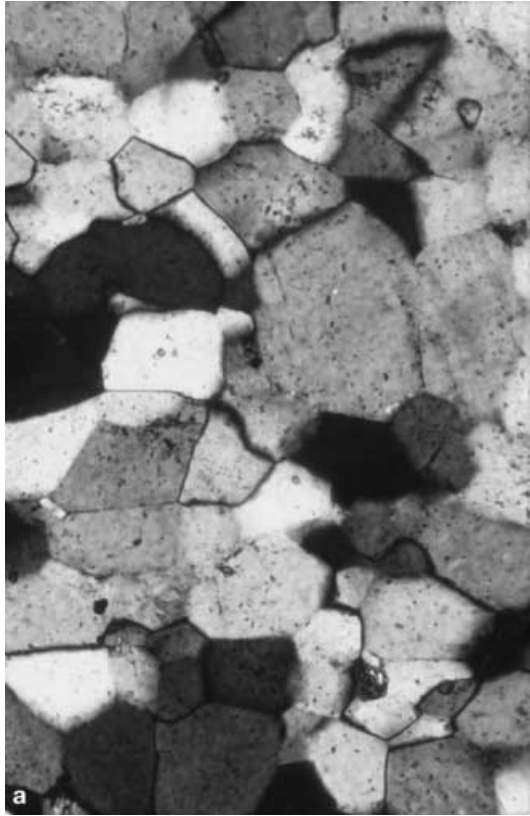


**Fig. 4a,b** Photomicrographs of foam textures. **a** Recrystallized and annealed plagioclase (~An<sub>25</sub>) from the Monte Rosa Ortho Gneiss, Val d'Ossola (Western Alps). Sample KR2686; long side of photograph=0.6 mm. **b** Recrystallized and annealed quartz from the Barrow chlorite zone near Dunoon, Grampian Highlands (Scotland). Sample KR1431B; long side of photograph=0.51 mm

### The development of grain boundary patterns during annealing

The grain boundary patterns of foam textures are qualitatively different for different times and temperatures of annealing. These differences are commonly registered through the frequency distributions of dihedral angles and the geometry of the boundaries.

#### Geometry of the grain boundaries

Figure 5 illustrates the development of camphor foam textures during several hours of normal grain growth at 60 °C. After 8 h of annealing, most boundaries have developed an apparent weak to strong curvature (Fig. 5A). However, a close examination with the universal stage reveals that these boundaries are not really curved but divided into two to several straight segments (facets) that are bridged by curved boundary sections of up to several microns long. Especially at

triple junctions, boundaries show short facets (Fig. 5A-a) but they also occur away from triple junctions (Fig. 5A-b), even with zigzag shapes (Fig. 5A-c). After a further 2 h of annealing the grain boundary configuration remains nearly unchanged (Fig. 5B). The sizes of a few grains are reduced, but most grain boundaries are stable, even those with facets of highly different orientations (Fig. 5B-a). Some dihedral angles that are clearly different from 120° (Fig. 5B-b) or zigzag-shaped boundaries (Fig. 5B-c) are preserved. Straight boundaries may be shifted perpendicular to their length orientation (Fig. 5B-d) or rotated. During such rotations, the shape of a boundary may be preserved (Fig. 5B-e), new facets may be formed (Fig. 5B-f) or old ones may be eliminated (Fig. 5B-g). Boundaries may migrate without affecting neighbouring boundaries. Grains may grow or shrink without much effect on the surrounding boundary configuration (Fig. 5B-h). Consequently, there are strongly unstable boundaries adjacent to absolutely stable boundaries. Migrated grain boundaries occur in clusters. This indicates that boundary migration at a certain point may trigger migration of surrounding boundaries, i.e. localized changes in grain boundary configuration develop a 'field of influence'. However, these 'fields' have sharp limits.

After another 11.5 h of annealing the grain boundary network is partly strongly shifted and altered (Fig. 5C). However, 'non-equilibrium' configurations may remain (Fig. 5C-a), may be shifted without con-

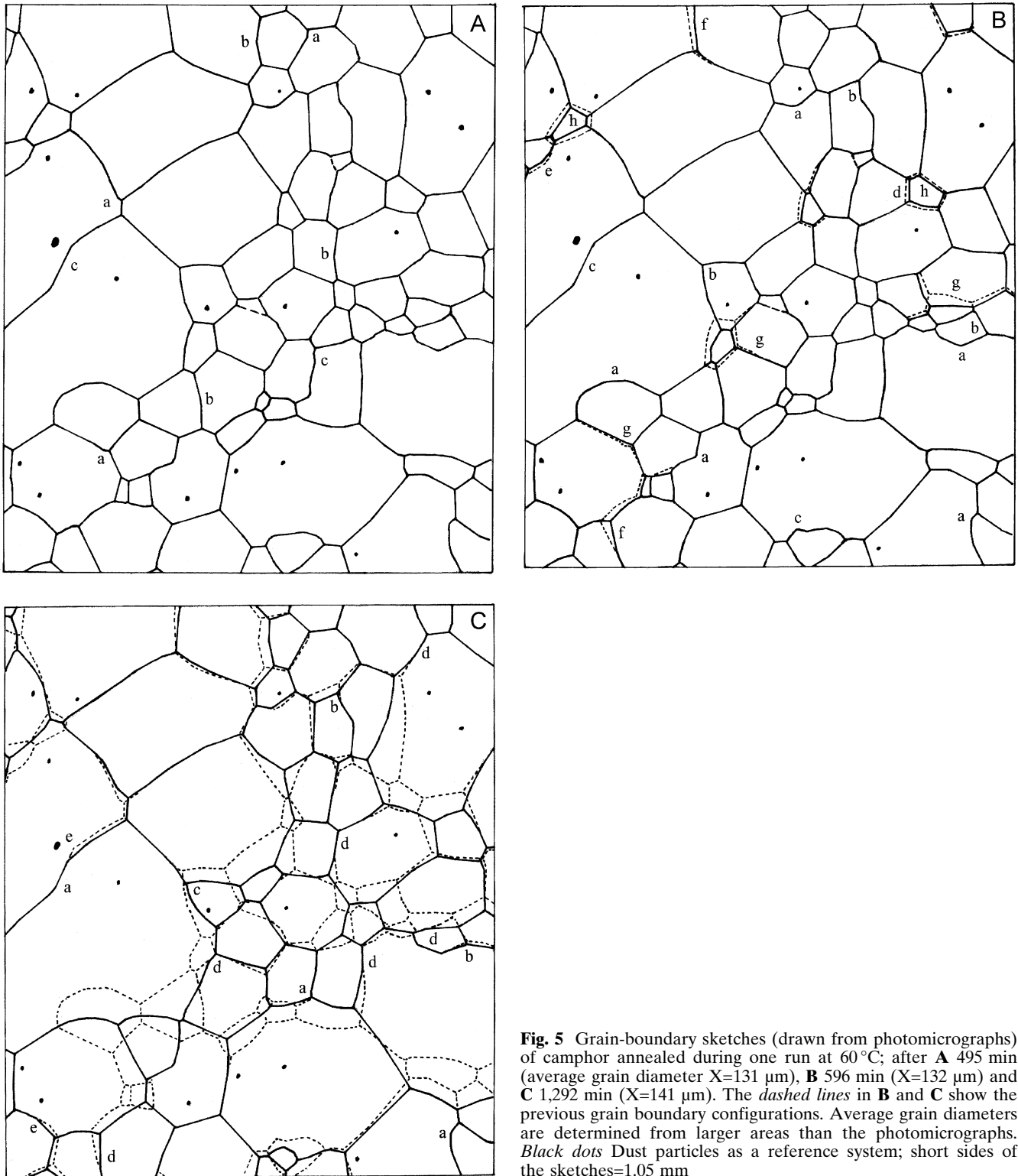


**Fig. 5** Grain-boundary sketches (drawn from photomicrographs) of camphor annealed during one run at 60 °C; after **A** 495 min (average grain diameter  $X=131\ \mu\text{m}$ ), **B** 596 min ( $X=132\ \mu\text{m}$ ) and **C** 1,292 min ( $X=141\ \mu\text{m}$ ). The *dashed lines* in **B** and **C** show the previous grain boundary configurations. Average grain diameters are determined from larger areas than the photomicrographs. *Black dots* Dust particles as a reference system; short sides of the sketches=1.05 mm

siderable changes (Fig. 5C-b) or even brought further away from 'equilibrium' (Fig. 5C-c). Boundaries may split into a 'kinked' and a stationary part (Fig. 5C-d) or the 'kink' migrates along the boundary (Fig. 5C-e). Even if major parts of the texture are affected there are still groups of stationary boundaries, mainly of

larger grains. In general, several grains have shrunk and a few others completely disappeared, resulting in a small increase in average grain size.

Even if the migration of grain boundaries in annealed rocks is not directly observable, all the grain boundary geometries found in analogue material also

occur in naturally annealed crystalline material such as the quartz aggregate shown in Fig. 4B. This suggests that at least in this respect the grain boundary geometry of the analogue material is not influenced by the thin-film shape of the material as well as by the two glass plates. A detailed survey of the grain boundary geometry by polarizing microscope and universal stage unravels geometry details as follows (Fig. 6): (1) short 3–5  $\mu\text{m}$  facets at triple junctions, (2) zigzag-shaped boundaries, and (3) groups of facets of slightly different orientation. Short facets at triple junctions are generally oriented in a way to form dihedral angles close to  $120^\circ$  but there are also facets that

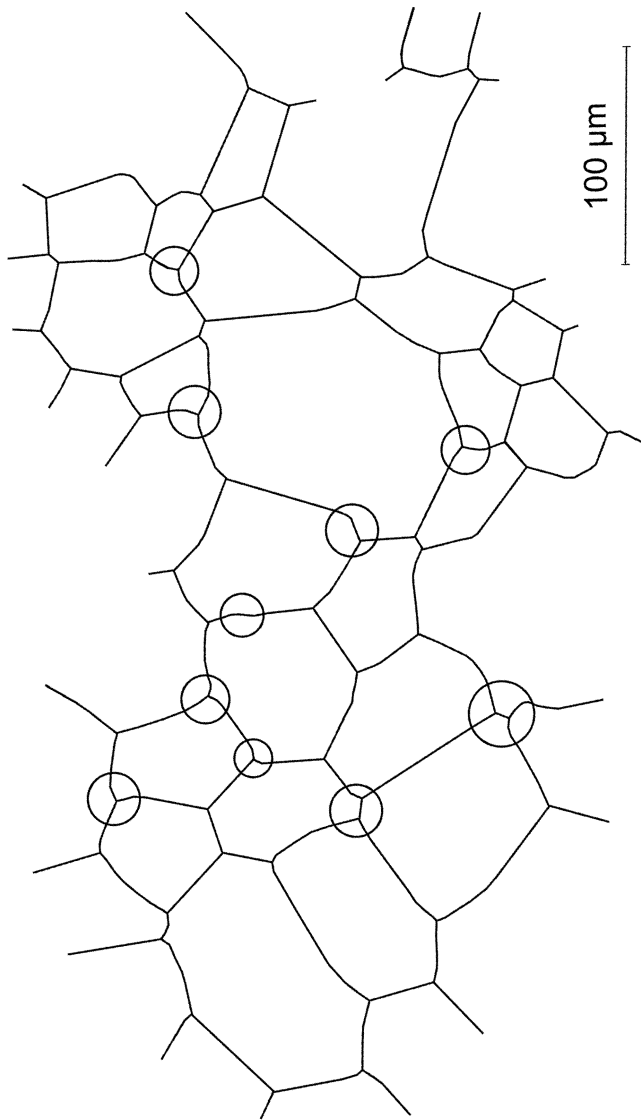


**Fig. 6** Grain boundary pattern of statically recrystallized and coarsened quartz; sample KR1431B, from the Barrow chlorite zone, near Dunoon, Grampian Highlands, Scotland; thin-section sketch. Circles indicate some of the numerous short boundary facets at triple junctions. The sketch does not exactly represent the boundary geometry in the thin-section plane but approximately the true angles at triple junctions, as deduced by rotating the section on the universal stage

lead to angles clearly different from  $120^\circ$ . With the aid of the universal stage all grain boundaries can be rotated to orientations perpendicular to the view plane. This procedure emphasizes the true shapes of the grain boundaries and explicitly shows that most, if not all, curved boundaries in reality consist of straight segments.

Figure 7 schematically illustrates the various types of grain boundary geometries that have been found in quartz and camphor grain aggregates. The 'equilibrium geometry', i.e. three straight boundaries meeting with approximately  $120^\circ$  dihedral angles (Fig. 7, type A), is a common feature but other boundary types are also common: short facets at triple junctions (types C and D), straight boundaries with dihedral angles far away from  $120^\circ$  (type B), boundaries composed of facets of clearly or only slightly different orientations (types G and H, or F, respectively) and two facets of approximately equal length (type E). Arrays of only slightly differently oriented facets can closely resemble a curved grain boundary, especially if the boundary is

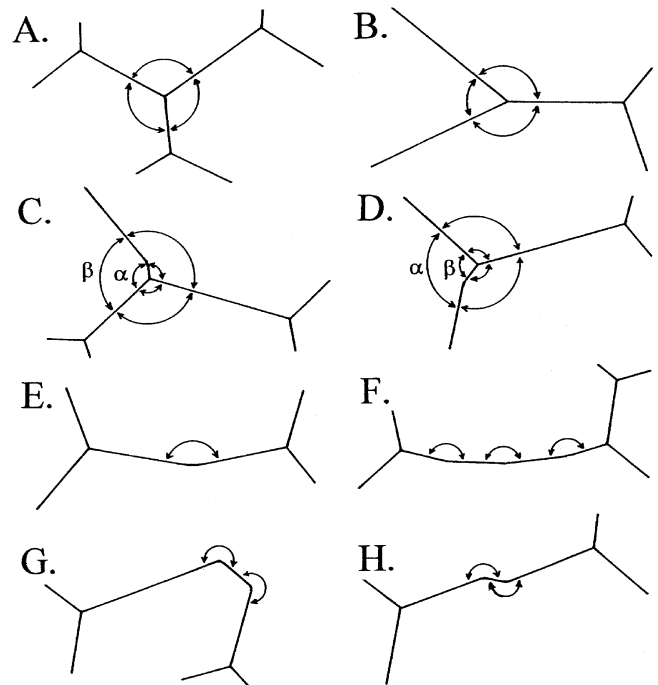


**Fig. 7** Principal types of 'stable' grain boundaries in experimentally and naturally annealed polycrystalline monophase material, as seen in two dimensions under the light microscope. Planar facets are connected by a short-distance curvature. *Type A* Planar boundaries meet at triple junctions with  $120^\circ$  or nearly  $120^\circ$  dihedral angles. *Type B* Planar boundaries meet with dihedral angles far away from  $120^\circ$ . *Type C* Boundaries form short facets at triple junctions to allow  $120^\circ$  angles (change from  $\beta$  to  $\alpha$ ). *Type D* Boundaries form short facets at a triple junction so that angles deviating from  $120^\circ$  are formed (change from  $\alpha$  to  $\beta$ ). *Type E* Boundary forms two approximately equally large facets between two triple junctions. *Type F* Boundary between two triple junctions forms several slightly misoriented facets. *Type G* Boundary between two triple junctions forms largely misoriented facets. *Type H* Boundary between two triple junctions forms a zigzag shape

oblique to the plane of view, which is the common situation under the polarizing microscope. An earlier study by Vernon (1968) presents and interprets many of the same features. In general, in the literature curved grain boundaries are reported; however, the photomicrographs or sketches of naturally or experimentally annealed crystalline material frequently exhibit the types of facets described in the present paper (e.g. Jessel 1986, Fig. 10a; Bons 1994, Figs. 2.7 and 4.8a). Especially TEM photographs on the scale of a few down to  $<1\ \mu\text{m}$  show a short curvature between straight segments (Gleiter 1969, Fig. 6; McDonnell 1998, Fig. 6.6c and e). However, these curvatures do not appear on the nanometre scale (Wolf and Merkle 1992).

### Dihedral angles at triple junctions

It is easy to determine the frequency distribution of dihedral angles in a foam texture. Transparent materials allow the true dihedral angles to be directly measured by the universal stage. However, in the case of 'curved' grain boundaries the angles are not unequivocally determinable. In the literature the measurement procedure is rarely described. According to Spry (1969, p. 168) the tangent lines to curved boundaries intersecting at a triple junction enclose the dihedral angle. This may provide the true angle in the case of straight boundaries or boundaries composed of facets of only slightly different orientation (Fig. 7, types E and F), but not if a straight boundary ends in a short facet of highly different orientation (Fig. 7, type C) which possibly is hardly detectable – especially if measurements are performed under the light microscope without a universal stage. Following Vernon (1968), the dihedral angles of the present study are based, if not indicated otherwise, on the grain boundary parts close to the triple junctions, measured with the universal stage. Angles from the annealed analogue material closely cluster around  $120^\circ$ , independent of the level of temperature and time of annealing (Fig. 8). The cumulative frequency curves strongly resemble those curves from statically recrystallized and coarsened plagioclase grains developed under granulite and lower amphibolite facies conditions (Fig. 9). Foam textures of quartz, statically recrystallized and coarsened under greenschist facies conditions show a similar distribution of dihedral angles (Fig. 10). However, the dihedral angles for grain boundary facets further away from the triple junctions cluster more weakly around  $120^\circ$  than those for facets close to the triple junctions. The cumulative curves do not give any indication that the dihedral angles depend on the temperature level of annealing.

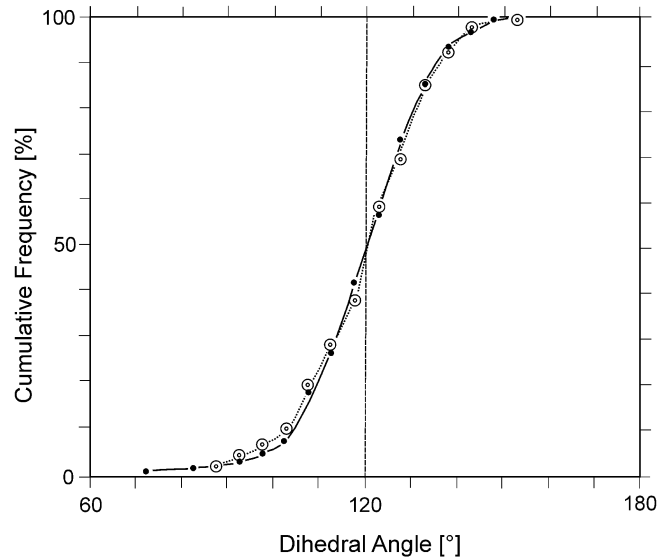


**Fig. 8** Cumulative frequency distribution of dihedral angles from annealed camphor powder. *Dots* 3,335 min annealing at  $23^\circ\text{C}$ , 184 measurements; *circles* 328 min annealing at  $60^\circ\text{C}$ , 122 measurements; true angles, determined by a universal stage

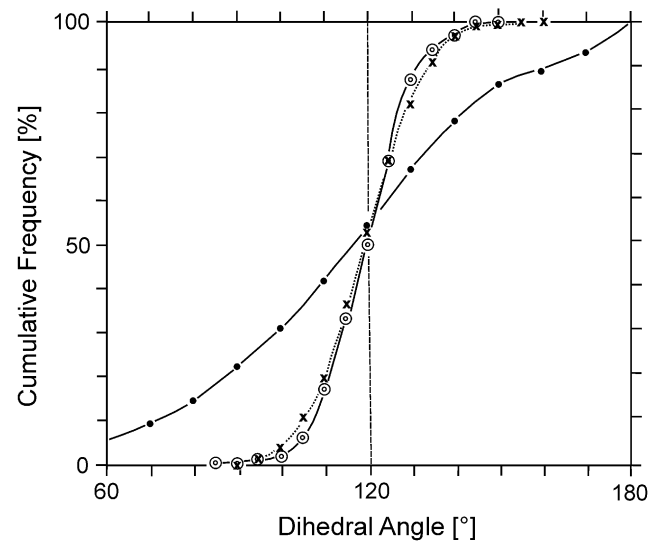


**Fig. 9** Cumulative frequency distribution of dihedral angles from statically recrystallized plagioclase grain aggregates and a diagenetic quartz-oolite. *Circles* Orthogneiss from the Sesia Zone (Western Alps); annealed at  $\sim 560^\circ\text{C}$  (Kruhl 1979); sample KR705; An $\sim$ 25; average grain size  $\sim 180\text{--}200\ \mu\text{m}$ ; 240 measurements. *Crosses* Granulite from the fossil Hercynian lower crust of Calabria (Italy); annealed at  $\sim 725^\circ\text{C}$  (Kruhl and Huntemann 1991); sample KR3265, An $\sim$ 50; average grain size  $\sim 400\ \mu\text{m}$ ; 240 measurements; *dots* quartz oolite, surface temperature, modified

### The crystallographic orientation of grain boundaries

It has been known for a long time that grain boundaries in mono-phase materials are crystallographically controlled under certain conditions. Voll (1969, p. 117)

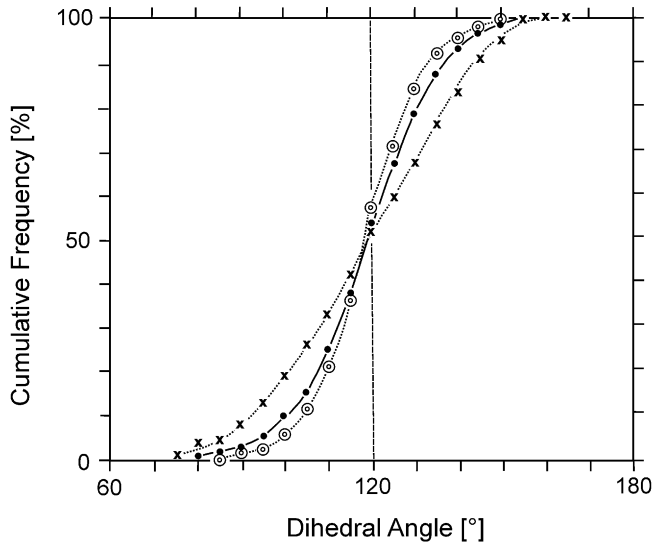


**Fig. 10** Cumulative frequency distribution of dihedral angles from statically recrystallized and coarsened quartz grain aggregates. Chlorite schist from the Barrow chlorite zone, near Dunoon, Grampian Highlands, Scotland; sample KR1431B. *Dots* All types of dihedral angles (as shown in Fig. 7); 862 measurements. *Circles* Angles between short boundary facets at triple junctions ( $\alpha$  in Fig. 7C); 206 measurements. *Crosses* Angles away from triple junctions ( $\beta$  in Fig. 7C), 208 measurements; true angles, determined by the universal stage

pointed to the fact that during deformation and strain-induced grain boundary migration the straight segments of sutured quartz–quartz boundaries are preferentially oriented along rhombohedral planes. This crystallographic control results in preferred frequencies of the angles between the poles of the segments and quartz-[c] ranging from  $\sim 40$  to  $70^\circ$ . Consequently, an approximately rectangular boundary pattern is developed that is especially common in rocks from high-grade metamorphic regions or from contact metamorphism (Voll 1969, Fig. 50; Gapais and Barbarin 1986, Fig. 4; Masberg et al. 1992, Fig. 3; Büttner and Kruhl 1997, Fig. 6d). Foam textures of quartz also consist of crystallographically oriented grain boundaries (Fig. 11A). The frequency orientation of the angles between the boundary poles and the [c]-axes of the neighbouring quartz crystals clearly differs from a uniform distribution. Specific maxima occur between  $\sim 30$  and  $80^\circ$ . On the basis of an estimated  $\pm 2^\circ$  accuracy of measurement for the [c]-axes and  $\pm 1^\circ$  for the boundary poles, the maxima shown in Fig. 10A are significant. The [c]-axis and the pole of a specific crystallographic plane enclose a specific angle. Under the premise that vice versa a specific angle indicates a specific crystallographic plane, the grain boundaries preferentially develop along specific rhombohedral but not basal and prism planes. Short boundary facets at triple junctions (Fig. 7, type C) also follow rhombohedral planes, but less commonly (Fig. 11B). The annealed analogue material does not allow the meas-

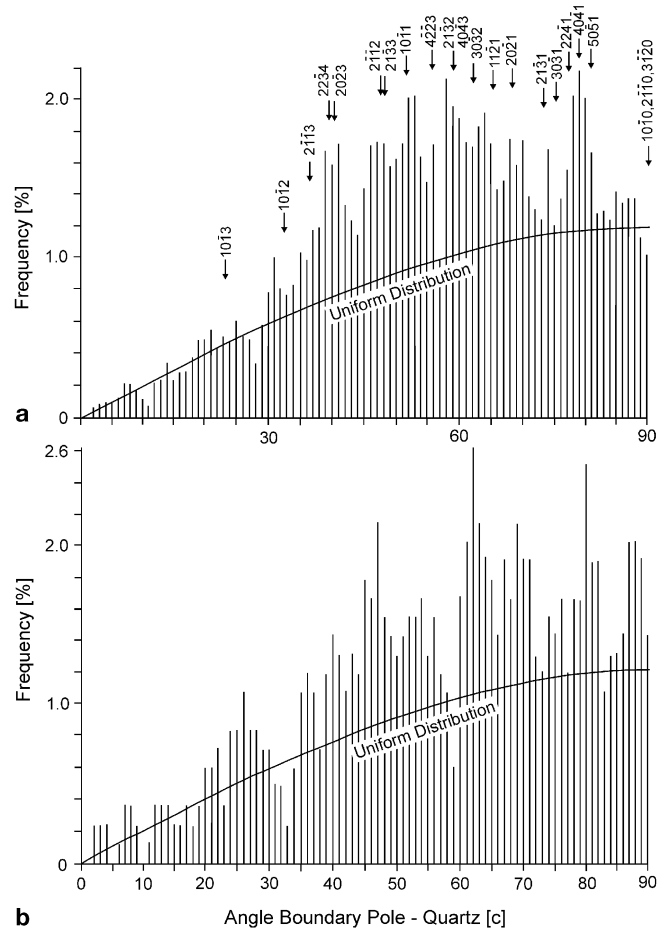


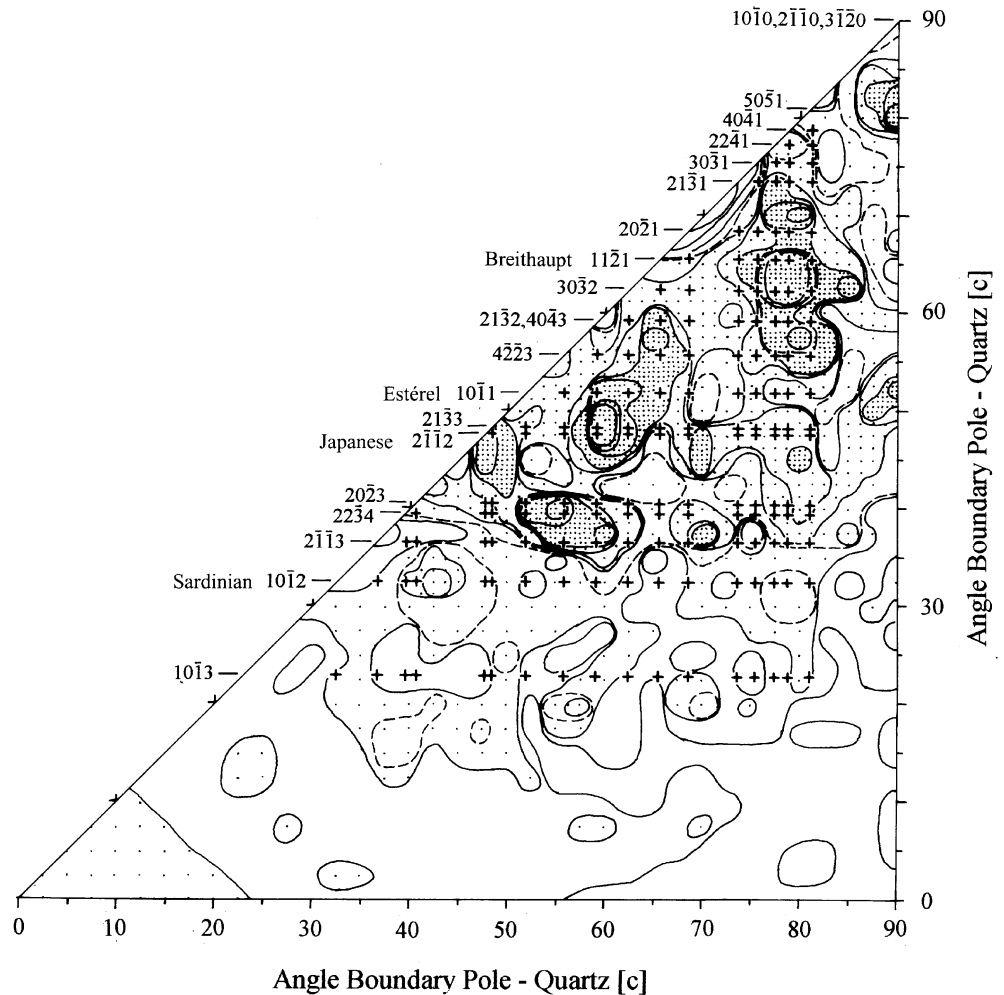
**Fig. 11a,b** Crystallographic orientation of grain boundaries and grain boundary segments, respectively, from statically recrystallized and coarsened quartz, Barrow chlorite zone, near Dunoon, Grampian Highlands, Scotland. Angle between boundary pole and [c] of both the neighbouring quartz grains versus frequency (percentage of total number of measurements); kriging over  $3^\circ$ . Principal crystallographic planes of quartz and the uniform distribution (distribution of equal probability = sine of the angle, times 1.3 – to allow an approximate fit with the frequency values of  $0$ – $30^\circ$  and  $80$ – $90^\circ$  in **a**, which is seen as the ‘background’ of the distribution) of any crystallographic position are indicated; sample KR1431B. **A** All types of boundaries, but without short facets near triple junctions (type C and D, Fig. 7); 1,326 measurements. **b** Short facets near triple junctions; 278 measurements

urement of grain boundary orientations because of the effect of the two glass plates, which forces many boundaries into a position perpendicular or nearly perpendicular to the plates – independently of the crystallographic orientations of the boundaries.

Considering the orientation of a grain boundary relative to both neighbouring crystals, specific pairs of boundary orientations commonly occur (Fig. 12). However, two dominant single orientations (Fig. 11A) do not necessarily form a significant pair of orientations. For example, the  $(10\bar{1}1)$  plane forms significant maxima solely together with  $(22\bar{3}4)/(20\bar{2}3)$ ,  $(21\bar{3}2)/(40\bar{4}3)$  and the (subordinate) prism planes, but



**Fig. 12** Angle between boundary pole and [c] of one neighbouring quartz grain versus angle between the boundary pole and [c] of the other neighbouring grain. 1,604 measurements; kriging over angles of  $5 \times 5^\circ$  with  $2.5^\circ$  steps; frequency distribution of all grain boundaries minus uniform distribution (as shown in Fig. 11). Isolines = 0.5 measurements per  $2.5 \times 2.5^\circ$ , starting with  $-1.5$  below up to  $+3$  above uniform distribution. Domains above  $-0.5$  are widely, above  $+0.5$  moderately and those above  $+1.5$  densely dotted. Dashed isoline = uniform distribution. The positions of principal crystallographic planes and their intersections are indicated



not together with the otherwise dominant  $(22\bar{4}1)$ ,  $(4041)$   $(5051)$  planes (Fig. 12). In addition, with the exception of  $(2\bar{1}\bar{1}2)$  and  $(21\bar{3}3)$ , the planes are not combined with themselves, i.e. rhombohedral planes (and prism and basal planes, too) do not preferentially form common boundaries between two neighbouring quartz crystals. If boundary facets are formed at triple junctions to allow a better approach to  $120^\circ$  angles there is a tendency to shift the facet poles away from the regions of higher frequency (Fig. 13). However, this is only a trend and the reverse may occur in single cases. Moreover, it should be pointed out that, despite the preferred crystallographic orientation of many boundaries parallel to low-index planes, a considerable number of boundaries appear to be oriented parallel to high-index or even irrational crystallographic planes. They partly build the random background of the frequency distribution in Fig. 11. Such a high background can be explained by the fact that the geometry of the foam texture will force certain grain boundaries into certain positions that may be of crystallographically high-index or even irrational, at least above the nanometre scale.

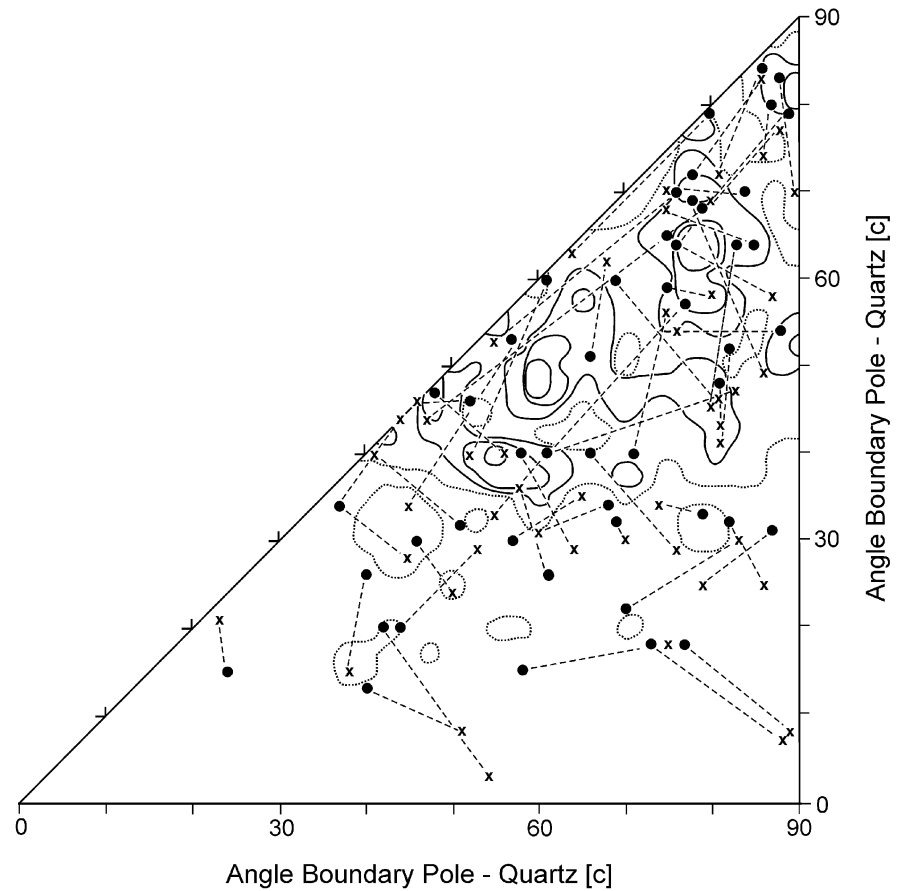
## Discussion

The shape, pattern and crystallographic orientation of grain boundaries represent important characteristics of crystalline material and its deformation and annealing history. Annealing, i.e. heating without deformation, is a comparatively simple but fundamental process in metamorphic rocks. Nevertheless, few data on annealed material are available. The present study concentrated on three easily accessible parameters for the characterization of annealed mono-phase material: (1) the grain size as a result of normal grain growth, (2) the dihedral angles at triple junctions, and (3) the crystallographic orientation of the boundaries.

### Normal grain growth

It is well known from metals, ceramics and metamorphic rocks that an aggregate of crystals increases in average grain size when heated at elevated temperatures (Spry 1969; Cotterill and Mould 1976; Kingery

**Fig. 13** Diagram as Fig. 12. Only the positions of large planar boundaries (*filled circles*) and short facets (*crosses*) near triple junctions and part of the isolines from Fig. 12 are presented. 49 pairs of measurements; type C boundary (Fig. 7). *Dotted isoline*=uniform distribution. With 22 pairs of measurements the large boundary is from a higher density domain than the short facet and with 15 pairs of measurements from a domain of the same density. Only 12 measurement pairs show the short facets in a relatively higher density position



et al. 1976; Joesten 1991). The reduction in grain-boundary area and, consequently, in total boundary energy is generally seen as the driving force for this grain growth, called 'normal growth'. At triple junctions the grain boundaries tend to meet at  $120^\circ$  (if all the grain boundaries are equal in energy, i.e. in isotropic material). Grains with side numbers different from six (in a two-dimensional section) form curved boundaries in order to keep the  $120^\circ$  dihedral angles. These curved boundaries migrate toward their centre of curvature. Consequently, grains with less than six sides tend to shrink and grains with more than six sides tend to grow larger. This process would lead to an infinite increase in average grain size but is balanced by other mechanisms that stop grain growth. Growth limitation can mainly arise from the existence of solute atoms, second phase particles and preferred crystallographic orientations (Cotterill and Mould 1976; Humphreys and Hatherly 1995; and references therein). Experiments on normal grain growth of rock-forming minerals and analogue materials indicate a continuous growth until stopped by second phase particles. On the other hand, there are experiments, including those on camphor described above, which indicate stabilization of grain size without such factors (see discussion in Kingery et al. 1976; Olgaard and Evans 1988; Covey-Crump and Rutter 1989; Joesten

1991). Studies on polycrystalline metals have shown the existence of an 'ultimate grain size' that usually depends on the composition and phase-structure of crystalline material and on the annealing temperature (Cotterill and Mould 1976, and references therein). The grain growth itself is seen as the grain-size stabilizing mechanism; it leads to a decreasing grain boundary area per unit volume and, consequently, to a decreasing grain boundary energy. Thus, a reduction in driving force that finally is no longer able to sustain further grain growth. Moreover, the results of the present study indicate that the crystallographic orientation of the grain boundaries may serve as an additional powerful mechanism to stabilize the grain size (see further below).

As established for metals, there also appears to be a rough correlation between the temperature of metamorphism and the average grain size of rock-forming minerals (Spry 1969, and references therein). Again, the present normal grain growth experiments indicate that the average grain size, stabilized after a certain period of annealing (Fig. 1), roughly correlates with the annealing temperature (Fig. 2). However, the correlation is quite weak. This points to additional factors influencing the 'equilibrium' grain size. Two well-known factors are (1) the grain size at the beginning of normal grain growth and (2) the nucleation rate,

which, again, is dependent on the temperature (Kingery et al. 1976, Chap. 10). Obviously, the period of loading of the camphor powder also influences the grain size (Fig. 2) as is indicated by different average grain sizes of experiments with different loading periods – possibly because of a higher number of nuclei after a longer period of loading.

The present measurements on naturally recrystallized and coarsened plagioclase grains indicate that grain sizes resulting from normal grain growth can be applied on a statistical basis as a geothermometer. Further indications of such an application of the size of recrystallized and coarsened grains are given in the literature. Voll (1980) reports size distributions of recrystallized quartz grains from the Aar and Gotthard Massif (central Alps) that reflect the zones of regional heat distribution during a late stage of the Alpine orogeny. Covey-Crump and Rutter (1989) present correlations between calcite grain size and the maximum temperature of metamorphism; however, they question these results in a later paper (Covey-Crump 1997). In the Western Alps, the isolines of equal grain size correlate with the isograds of regional metamorphism (Altenberger et al. 1987). Such a correlation would not exist if for example pinning second phases would dominantly influence the final grain size during annealing. Concerning the grain-size thermometer, it is important that the experiments on camphor indicate a rapid stabilization of grain sizes even at annealing temperatures of not more than 10% of the melting temperature (Fig. 1). This suggests that the annealing grain size can be considered as a parameter that is independent of the period of regional metamorphism, even if this has not been explicitly proved for metamorphic rocks.

#### Dihedral angles at triple junctions

Dihedral angles are considered as a measure of equilibration. Compared with metamorphic rocks, in diagenetic rocks the dihedral angles of quartz and calcite cluster less closely at  $\sim 120^\circ$  and show nearly a random distribution (Fig. 8; Voll 1969, Fig. 52). Optically visible dihedral angles of equilibrium values have been used in a limited sense as evidence of textural equilibrium (Holness et al. 1991). On the basis of simulations of dihedral angles, it has been suggested that one should take the cumulative frequency curves as a measure of textural equilibration (Elliot et al. 1997). The present study does not indicate differences between dihedral angles from material annealed at different temperatures over different times, experimentally or naturally. A problem arises if the short boundary facets at triple junctions are not included in the measurements. In that case, the angles cluster much more broadly at  $\sim 120^\circ$  (Fig. 9). It is crucial that very short facets may be not visible because they are inclined to the plane of view or because they are of

submicroscopic scale. Consequently, it is not possible to measure dihedral angles in a comparable way. The frequency distribution curves of dihedral angles may indeed help to distinguish between annealed and non-annealed polygonal textures, but they appear to be unsuitable to give more detailed information about the degree of textural equilibrium in crystalline material.

#### The crystallography of grain boundaries

On the basis of equant and polygonal grain shapes and of dihedral angle distributions clustered closely around  $120^\circ$ , it has been concluded that the anisotropy of grain boundary energy of quartz or feldspars has only a minor effect on the grain boundary configuration in grain aggregates of these minerals. Nevertheless, there is at least a small dependency of the grain boundary energy on the crystallographic orientation (Vernon 1968; Spry 1969). The present study provides indications that, in more detail, during normal grain growth there is a clear and very specific effect of the crystallographic orientation not only on the shape and orientation of grain boundaries but also on the development of a foam texture. Indications are:

1. In foam textures the grain boundaries between two triple junctions are commonly composed of two or several planar facets of mostly slightly different orientation (Figs. 5 and 6).
2. Even neighbouring facets of highly different orientation and dihedral angles deviating significantly from the 'equilibrium angle' of  $120^\circ$  may be stable over long periods of annealing (Fig. 5).
3. The boundary facets preferentially occupy specific crystallographic orientations (in the case of quartz they are rhombohedral; Fig. 11A) in relation to both neighbouring crystals (Fig. 12).
4. Even short facets at triple junctions may occupy preferred crystallographic orientations (Fig. 11B), however, on average less significantly.

These observations suggest that the preferred crystallographic orientations shown in Fig. 11 are low-energy positions that are favoured during grain coarsening. However, the situation is probably more complicated. Grain boundaries from quartz foam textures are commonly orientated parallel to low-index rhombohedral planes, but not universally (Figs. 11 and 12) and not parallel to the basal and prism planes, although the latter low-index planes should represent relatively 'stable' orientations. Moreover, coherent planes with coincidence atoms do not appear to prevail. This is indicated by the fact that the angles between the boundary poles and [c] of the two neighbouring crystals are not more frequently of equal size than uniform distribution, i.e. that grain boundaries do not occupy planes of symmetry relative to both neighbouring crystals more frequently than the uniform distribution (Fig. 12). Twin boundaries, too, do not rep-

resent preferred grain boundary positions. Only the mirror planes of Japanese twins occur statistically dominantly but not those of Sardinian, Estérel and Breithaupt twins (Fig. 12). Based on electron microscope studies it has been shown that coherent boundaries in metals generally do not contain coincidence atoms (Gleiter 1982). If this is also true for non-metallic minerals it could explain the relatively low stability of coherent boundaries in the investigated foam textures. On the other hand, more recent high-resolution electron microscope studies on metals and ceramics show that planar boundary facets also occur on the nanometre scale (Norton and Carter 1992; Wolf and Merkle 1992). These facets are preferentially oriented parallel to low-index planes. Moreover, high-index planes or planes of irrational positions may be formed by small-scale atomic steps parallel to low-index planes. In general, it has been demonstrated for metals that there is a tendency of the atomic structure to preserve a high degree of atomic-level coherency across any type of interface between two grains (Wolf and Merkle 1992). By this observation the possibility arises that also in such a complex crystal structure like that of quartz, a high degree of coherency occurs even for asymmetric orientations of the boundary and the neighbouring crystals relative to each other.

Moreover, the relationship between the crystallographic orientation and the energy and, therefore, the relative stability of grain boundaries may be complicated in so far as the energy at least of high-angle boundaries appears to be sensitive to many different factors like the electron bond structure, solute segregation, saturation of bonds in covalent solids and electrostatic energy in ionic materials and not only to the geometric relationship across an interface (Palumbo and Aust 1992). From this viewpoint, simple microscope investigations on the occurrence of different grain boundary orientations under different natural conditions may provide useful data on relative grain boundary energies and, therefore, on the development of grain boundary patterns in crystalline material.

In addition, models on the mobility of grain boundaries have to take into account the fact that most, if not all, 'curved' boundaries are not really curved but form several distinct planar facets. The observed lack of curvatures of grain boundaries eliminates the basis of all models that include such curvatures. For example, equations such as  $F=2\gamma/r$  ( $F$ =driving force,  $\gamma$ =grain boundary energy per unit area of boundary,  $r$ =mean radius of curvature, McLean 1957) which predict a high driving force for strongly curved boundaries cannot hold for the type of grain boundary consisting of two or several planar facets. Moreover, it has been discussed and pointed out by Cotterill and Mould (1976, p. 284) that it is not the reduction of grain-boundary curvature but the reduction of total area of grain boundaries that provides the overall driving force for grain growth. This view is supported by the observation that networks of straight bound-

daries and boundary facets without clear curvature stay mobile during annealing (Fig. 5). In this respect it is important not to consider grain boundaries as isolated parts of a texture that are immobile if occupying low-energy positions. The intersection line of two 'stable' boundaries restricts the position of the third boundary, which can only rotate around this line. Therefore, the stability of a boundary or a boundary facet not only depends on its own energy level but also on the energy levels and the geometry of the surrounding boundaries, as is also indicated by observations on analogue materials (Fig. 5). In general, the presented observations suggest that during normal grain growth an increasing number of grain boundaries reach relatively stable positions (mainly dependent on their crystallographic orientation but probably also on their structure and other factors), thus leading to a decrease of grain boundary mobility and, finally, to a cessation of grain boundary migration.

On a statistical basis, it has been shown that dihedral angles at short boundary facets (Fig. 7, type C) are closer to 120° than for the other grain boundaries (Fig. 10). On one hand, the tendency to form 120° angles at triple junctions appears to dominate the effect of crystallographic orientation. On the other hand, there are numerous short facets at triple junctions with specific crystallographic (i.e. rhombohedral for quartz) orientations but with dihedral angles strongly deviating from 120° (Fig. 7, type D).

In general, a comparison between mineral and soap foam textures may be misleading because there is a strong effect of the crystallographic anisotropy on the development of grain boundary patterns. In this context it appears doubtful if theories on normal grain growth and related computer simulations (see e.g. review by Atkinson 1988) are meaningful if they do not consider the crystallographic anisotropy of crystalline material.

---

### Concluding remarks

The main results of the present study are:

1. On a statistical basis, during natural as well as experimental annealing, grain sizes stabilize at certain values that can be applied as a geothermometer.
2. The frequency distribution of dihedral angles from annealed material is independent of the time and temperature of annealing. The average value of these angles is ~120°. but they can deviate significantly from this value and form geometrically 'non-equilibrium' configurations, even after long periods of annealing.
3. On the light-microscope scale most, if not all scales, 'curved' grain boundaries consist of planar boundary facets of slightly different orientation. This observation is backed by observations on the

nanometre scale that again show planar boundary facets (Norton and Carter 1992; Wolf and Merkle 1992).

4. Planar boundaries and boundary facets preferentially occupy distinct crystallographic orientations in relation to both neighbouring crystals. The same is true for short facets at triple junctions even if they show a slightly weaker crystallographic control.
5. During annealing, parts of a foam texture may become unstable while other parts remain stationary. In detail, even parts of a single boundary may remain stationary whereas others parts migrate. Migration may lead to a local textural disequilibrium or to an increase in disequilibrium.

In general, it follows that the anisotropy of surface energy has much influence on the development of foam textures and that models of texture development during grain coarsening should include the influence of the crystallographic orientation of grain boundaries. In this context it appears important to relate the orientation data to the geometry and pattern of the boundaries. Only a multivariate combination of such data sets will help to unravel the complex processes during the development of foam textures. A key position is held by the term 'textural equilibrium'. This term is not unequivocally defined. In the literature it is mostly used to imply that after a 'long' period of annealing the texture of crystalline material reaches a permanent state of 'balance' of specific microfabrics (e.g. 120° dihedral angles). In addition, the term 'textural equilibrium' is linked to the term 'minimum of energy'. However, it has been repeatedly pointed out that a 'geometric equilibrium' is not equivalent to an energy minimum (Spry 1969; Cotterill and Mould 1976). In any case, the complexity of foam texture development, as shown in the present study, indicates that minimizing the energy of the system does not mean minimizing the total grain boundary area because of the influence of the crystallographic orientation of grain boundaries. The texture has to be considered as a system of several, partly independent variables, e.g. the geometry of distinct boundaries, their internal structure, their orientation to each other, their crystallographic orientation with respect to both neighbouring grains and the internal structure of the neighbouring grains. This system possibly behaves in a non-linear way. It is conceivable that foam textures represent metastable systems or systems that oscillate around metastable states. In other words, grain boundaries may mutually influence each other and small changes may have a great effect on specific regions of the texture but without a permanent change of its general appearance. In such a case foam textures in particular, and possibly grain boundary systems in general, would represent systems in a condition of self-organized criticality (Bak et al. 1988).

**Acknowledgements** I wish to thank Matthias Nega and Ron Vernon for fruitful comments and Klaus Haas for the prepara-

tion of the electronic figure versions. The detailed reviews of two anonymous colleagues are gratefully acknowledged. The study was funded by the German Research Council (DFG) under grant Kr691/17.

## References

- Altenberger U, Hamm N, Kruhl JH (1987) Movements and metamorphism north of the Insubric Line between Val Loana and Val d'Ossola (Italy). *Jahrb Geol B-A Wien* 130:365–374
- Atkinson HV (1988) Theories of normal grain growth in pure single phase systems. *Acta Metall* 36:469–491
- Bak P, Tang C, Wiesenfeld K (1988) Self-organized criticality. *Phys Rev A* 38:364–374
- Bons PD (1994) Experimental deformation of polyphase rock analogues. *Geologica Ultrajectina* 110, Universiteit Utrecht
- Büttner S, Kruhl JH (1997) The evolution of a late-Variscan high-T/low-P region: the southeastern margin of the Bohemian Massif. *Geol Rundsch* 86:21–38
- Cotterill P, Mould PR (1976) *Recrystallization and grain growth in metals*. Surrey Univ Press, London
- Covey-Crump SJ (1997) The normal grain growth behaviour of nominally pure calcite aggregates. *Contrib Mineral Petrol* 129:239–254
- Covey-Crump SJ, Rutter EH (1989) Thermally-induced grain growth of calcite marbles on Naxos Island, Greece. *Contrib Mineral Petrol* 101:69–96
- Dean JA (ed) 1985 *Handbook of chemistry*. McGraw-Hill, New York
- Elliot MT, Cheadle MJ, Jerram DA (1997) On the identification of textural equilibrium in rocks using dihedral angle measurements. *Geology* 25(4):355–358
- Gapais D, Barbarin B (1986) Quartz fabric transition in a cooling syntectonic granite (Hermitage Massif, France). *Tectonophysics* 125:357–370
- Gleiter H (1969) The mechanism of grain boundary migration. *Acta Metall* 17:565–573
- Gleiter H (1982) On the structure of grain boundaries in metals. *Mater Sci Eng* 52:91–131
- Holness MB, Bickle MJ, Graham CM (1991) On the kinetics of textural equilibration in forsterite marbles. *Contrib Mineral Petrol* 108:356–367
- Humphreys FJ (1997) A unified theory of recovery, recrystallization and grain growth, based on the stability and growth of cellular microstructures – I. The basic model. *Acta Mater* 45:4231–4240
- Humphreys FJ, Hatherly M (1995) *Recrystallization and related annealing phenomena*. Pergamon, Oxford
- Hunziker JC, Desmons J, Hurford AJ (1992) Thirty-two years of geochronological work in the Central and Western Alps. *Mémoires de Géologie, Lausanne*, vol 13
- Jessel MW (1986). Grain boundary migration and fabric development in experimentally deformed octachloropropane. *J Struct Geol* 8:527–542
- Jessel MW, Bons PD, Evans L, Barr TD (1999) Elle: a system for the simulation of deforming and metamorphosing rocks and its application to anisotropic grain growth. *Int Conf 'Deformation Mechanisms, Rheology, Microstructures'*, Neustadt, Book of Abstracts, vol 95
- Joesten RL (1991) Kinetic of coarsening and diffusion-controlled mineral growth, ch 11. *Rev Mineral, Min Soc Am*, vol 26
- Kingery WD, Bowen HD, Uhlmann DR (1976) *Introduction to ceramics*. Wiley, New York
- Kretz R (1966) Interpretation of the shape of mineral grains in metamorphic rocks. *J Petrol* 7:68–94
- Kruhl JH (1979) Deformation and metamorphism of the southwestern Finero Complex (Ivrea-Zone, N Italy) and the northerly adjacent gneiss zone (in German). PhD Thesis, University of Bonn

- Kruhl JH, Huntemann T (1991) The structural state of the former lower continental crust in Calabria (S. Italy). *Geol Rundsch* 80:289–302
- Masberg HP, Hoffer E, Hoernes S (1992) Microfabrics indicating granulite-facies metamorphism in the low-pressure central Damara Orogen, Namibia. *Precambrian Res* 55:243–257
- McDonnell RD (1998) Deformation of fine-grained synthetic peridotite under wet conditions. *Geologica Ultraiectina* 152, Universiteit Utrecht
- McLean D (1957) *Grain boundaries in metals*. Clarendon Press, Oxford
- Norton MG, Carter CB (1992) Grain and interphase boundaries in ceramics and ceramic composites. In: Wolf D, Yip S (eds) *Materials interfaces*. Chapman & Hall, London, pp 151–189
- Olgaard DL, Evans B (1986) Effect of second-phase particles on grain growth in calcite. *J Am Ceram Soc* 69:C272–C277
- Olgaard DL, Evans B (1988) Grain growth in synthetic marbles with added mica and water. *Contrib Mineral Petrol* 100:246–260
- Palumbo G, Aust KT (1992) Special properties of  $\Sigma$  grain boundaries. In: Wolf D, Yip S (eds) *Materials interfaces*. Chapman and Hall, London, pp 190–211
- Schenk V (1990) The exposed crustal cross section of southern Calabria, Italy: structure and evolution of a segment of Hercynian crust. In: Salisbury MH, Fountain DM (eds) *Exposed cross-sections of the continental crust*. Kluwer, Dordrecht, pp 21–42
- Smith CS (1948) Grains, phases and interfaces: an interpretation of microstructure. *Trans Am Inst Min Metall Eng* 175:15–51
- Spry A (1969) *Metamorphic textures*. Pergamon, New York
- Vernon RH (1968) Microstructures of high-grade metamorphic rocks at Broken Hill, Australia. *J Petrol* 9:1–22
- Voll G (1969) Klastische Mineralien aus den Sedimentserien der Schottischen Highlands und ihr Schicksal bei aufsteigender Regional- und Kontaktmetamorphose. Habilitationsschrift, Fak Bergb Hüttenw, TU Berlin, D83
- Voll G (1976) Recrystallization of quartz, biotite and feldspars from Erstfeld to the Leventina Nappe, Swiss Alps, and its geological significance. *Schweiz Mineral Petrogr Mitt* 56:641–647
- Voll G (1980) Ein Querprofil durch die Schweizer Alpen vom Vierwaldstätter See zur Wurzelzone – Strukturen und ihre Entwicklung durch Deformationsmechanismen wichtiger Minerale. *N Jahrb Geol Paläont Abh* 160:321–335
- Wolf D, Merkle KL (1992) Correlation between the structure and energy of grain boundaries in metals. In: Wolf D, Yip S (eds) *Materials interfaces*. Chapman & Hall, London, pp 87–150.
- Yager WA, Morgan SO (1935) Transitions in camphor and chemically related compounds. *J Am Chem Soc* 57:2071–2078